

Copyright
by
Jodi Lynette Wheeler
2011

**The Report Committee for Jodi Lynette Wheeler
Certifies that this is the approved version of the following report:**

**Fractals:
An Exploration into the Dimensions of Curves and Surfaces**

**APPROVED BY
SUPERVISING COMMITTEE:**

Supervisor:

Efraim Armendariz

Mark Daniels

Fractals:
An Exploration into the Dimensions of Curves and Surfaces

by

Jodi Lynette Wheeler, B.S.

Report

Presented to the Faculty of the Graduate School of

The University of Texas at Austin

in Partial Fulfillment

of the Requirements

for the Degree of

Master of Arts

The University of Texas at Austin

August, 2011

Dedication

To David, Samuel, Stewart and Isaac, my husband and children; their ongoing support and self sufficiency is what made my education possible. My dear husband, David, was cooking dinner and running a taxi service for the many soccer practices that I missed on the days I had to be at school, allowing me to write papers, study and spend endless hours with my head buried in research. My children also stepped up to help by doing their own laundry and much of the daily house work.

Without their unwavering support and love, it would not have been possible for me to earn my Masters or complete this report.

Acknowledgements

To Dr. Sandy Norman, for never telling us exactly what he expected from us in College Geometry, History of Math and Computer Math Topics, but instead encouraging his students to be creative and show him something new that he had not thought of before.

To Dr. Efraim Armendariz, for being the understanding “good cop” that encouraged me to believe I was smarter and more capable than I knew.

To Dr. Mark Daniels, for being the task master “bad cop” that kept me on track and was always concerned about quality of work and deadlines of assignments.

To my whole cohort of classmates, especially the Rotherettes, Katherine Garrett, Carmen Finch, Stephanie Foster and Darlene Sugarek; the marathon sessions of homework, group studying and Mojito night made every day at San Jack a special time to cherish.

August, 2011

Abstract

Fractals:

An Exploration into the Dimensions of Curves and Surfaces

Jodi Lynette Wheeler, M.A.

The University of Texas at Austin, 2011

Supervisor: Efraim Armendariz

When many people think of fractals, they think of the beautiful images created by Mandelbrot's set or the intricate dragons of Julia's set. However, these are just the artistic stars of the fractal community. The theory behind the fractals is not necessarily pretty, but is very important to many areas outside the world of mathematics.

This paper takes a closer look at various types of fractals, the fractal dimensionality of surfaces and chaotic dynamical systems. Some of the history and introduction of creating fractals is discussed. The tools used to prevent a modified Koch's curve from overlapping itself, finding the limit of a curves length and solving for a surfaces dimensional measurement are explored. Lastly, an investigation of the theories of chaos and how they bring order into what initially appears to be random and

unpredictable is presented. The practical purposes and uses of fractals throughout are also discussed.

Table of Contents

List of Figures	ix
List of Illustrations	x
Chapter 1 Introduction.....	1
Chapter 2 Creation of Fractals.....	3
Chapter 3 A Variation of Koch's Curve	7
Chapter 4 Methods of Measuring Fractal Dimensionality	12
Chapter 5 Chaotic Dynamical Systems	19
Chapter 6 Conclusion	24
References.....	25
Vita	26

List of Figures

Figure 1:	Classical von Koch curve.	7
Figure 2:	The $(5, 0.20)$ -von Koch curve.	8
Figure 3:	The $(5, \overline{0.33})$ -von Koch curve..	8
Figure 4:	The odd- n (n, c) -von Koch Curve Approximates an Isosceles Trapezoid	9
Figure 5:	The Tube Around a Triangle.....	15
Figure 6:	Cartioid Formed by Applying $f(z) = z^2$ to a Circle..	22

List of Illustrations

Illustration 1:	View of a Phoenix Fractal with $D:[0.60,0.64]$ & $R:[0.45,0.48]$.	3
Illustration 2:	View of a Mandelbrot Set..	4
Illustration 3:	View of a Phoenix Fractal.....	5
Illustration 4:	Drawing that Represents One Fixed Point in I ..	20
Illustration 5:	Drawing that Represents an Attracting Fixed Point.	20

Chapter 1: Introduction

In the late 19th and early 20th centuries, George Cantor, Helge von Koch and Giuseppe Peano were a few of the first mathematicians to draw curves unlike any other that had been created before. These curves were made using a process of iteration and were undifferentiable anywhere along the curve. When evaluated in smaller and smaller regions, they were found not only to be self similar, meaning that they appeared to have similar attributes, but to have an infinitely smaller and smaller detail. Now called *fractals* these confusing curves were originally referred to as “monsters” or “pathological” leaving most mathematicians unable and unwilling to work with them [6, p. 3].

The advent of high-speed computers that could generate literally millions of solutions for the points of these curves allowed Benoit Mandelbrot, a researcher at IBM, to create the beautifully detailed images now known as the Mandelbrot set. Many others have since followed and special software now makes it possible for virtually anyone to create an infinite number of fractal images.

Many systems found in the natural sciences, physics and world markets have typically been approximated using linear models, when of course these systems are anything but linear. Using fractal mathematics to analyze these chaotic systems is now allowing scientists and economists to find more accurate solutions and make better predictions within these dynamic systems.

While one can think of a surface as being flat, it is anything but flat when closely examined. A sheet of polished metal feels smooth to the touch, however zoom in at a microscopic level and the surface changes into a system of self similar pits and valleys resembling the landscape of a mountain range more than that of a mirror polished

surface. Similarly, when one looks at a forest's canopy, the repeating dips and bulges that are formed by various species of flora and fauna that live in the forest create a visually smooth surface when observed from a far enough distance.

Analyzing a curve's or surface's dimensionality for roughness or smoothness has been important to many areas of science and industry. The length of a coastline's edge depends on the measure of its fractal dimension. Plastic wrap with a very smooth surface will be more resistant to bacterium clinging to its surface and reduce the spread of illness; while the texture of a forest's canopy can give real evidence as to its health. Using fractal methodology to measure the roughness or smoothness of a curve or surface, allows measure of these edges and surfaces to be analyzed in such a way that an extensively detailed and clear result can be counted on to be true and accurate.

Chapter 2: Creation of Fractals



Illustration 1. View of a Phoenix fractal with $D:[0.60,0.64]$ & $R:[0.45,0.48]$.

Intricate and beautiful images like the one seen in Illustration 1 are why many people are initially drawn to the study of fractals. Illustration 1 is a very small area of the Julia set from the iterated equation

$$z_{n+1} = z_n^2 + p + qz_{n-1},$$

which will be discussed and defined in this chapter [7, p. 250].

All mathematically produced fractals are formed through a process of *iteration*, which is a method of using a function's previous output as its new input. This process causes a function's range to become its domain as well. For example, if x_0 is the *seed* or original input value, then $x_1 = f(x_0)$ and $x_2 = f(x_1)$ then the process is repeated for the required number of iterations, thus the range becomes the domain of the function.

The iteration of a simple polynomial $f(x) = x^2 - 0.5$ with a seed value of $x_0 = 0.7$ computes the following sequence.

$$x_0 = 0.7$$

$$x_1 = f(0.7) = 0.7^2 - 0.5 = -0.01$$

$$x_2 = f(-0.01) = (-0.01)^2 - 0.5 = -0.4999$$

$$x_3 = f(-0.4999) = (-0.4999)^2 - 0.5 = -0.25009999$$

$$x_4 = f(-0.25009999) = (-0.25009999)^2 - 0.5 = -0.437449995$$

The output values appear to be random, however, if this iteration process is continued, these values will eventually approach -0.366025 , bringing order to the function and showing it to be chaotic rather than random.

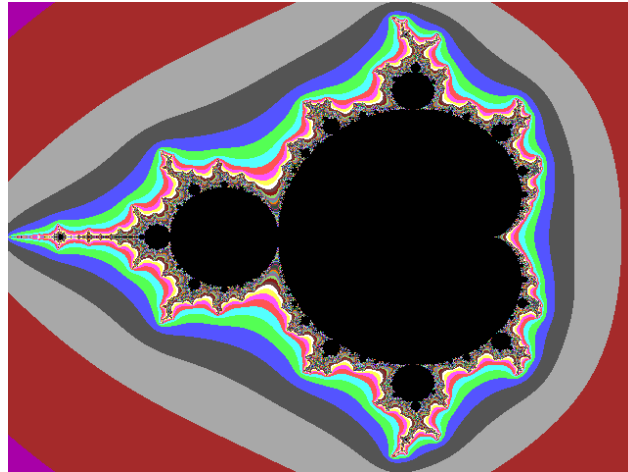


Illustration 2. View of Mandelbrot set computer rendered in the complex plane.

The Mandelbrot set is a deceptively simple looking equation graphed in the complex plane,

$$z_{n+1} = z_n^2 + c$$

where z and c are both complex numbers in the form $a + bi$ and $z_0 = c$. As the equation is iterated, some of the values will converge to a complex value, some will diverge to infinity and others will settle on attracting fixed points. Using computer software, the

values that converge to a complex value are traditionally colored black. While those that diverge to infinity can be thrown out, leaving only the attracting fixed points behind. This is what creates the initial outline of the Mandelbrot cardioid shown in Illustration 2. Different colors are then assigned to the divergent values based on how quickly they diverge out of the set, giving the fractal its interesting color variations as the equation is repeatedly iterated.

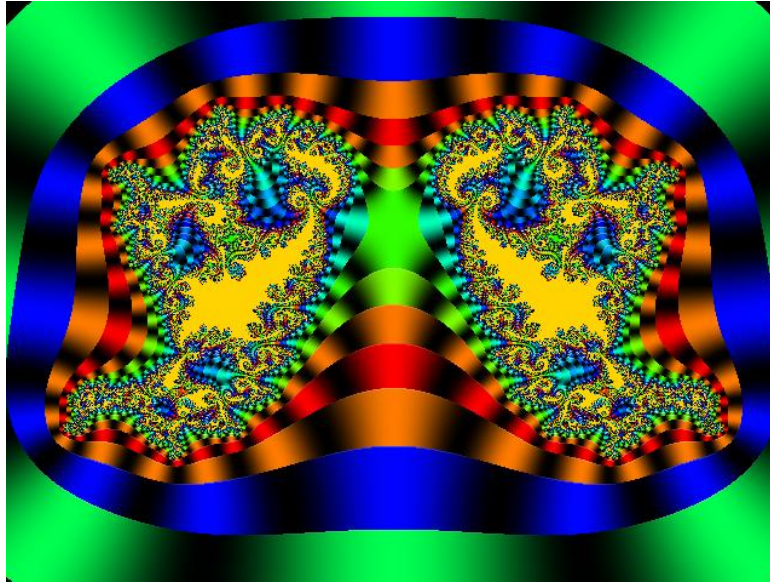


Illustration 3. View of Phoenix fractal computer rendered in the complex plane.

The Phoenix fractal, as shown in Illustrations 1 and 3, was discovered by Shigehiro Ushiki at Kyoto University. It is a transformation of the basic Mandelbrot equation

$$z_{n+1} = z_n^2 + c$$

into

$$z_{n+1} = z_n^2 + p + qz_{n-1}$$

where both the current and the previous value of z are used at the same time. Also, p is the real part of c and q is the imaginary part of c [7, p. 250]. In addition, the rendering must also be turned 90° or the phoenixes will be laying on their sides above and below each other rather than side by side as seen in Illustration 3.

This has been just a small sample of the many exquisite images that have been made using iterated equations. The mathematics behind these images will be examined more closely in Chapter 5.

Chapter 3: A Variation of Koch's Curve

Keleti and Paquette have examined the modified Koch curve by replacing the familiar equilateral triangle in the center one-third of the base line segment, as in Figure 1, with an n -gon, in the center of the base line segment taking up a portion, c of that segment such that $0 < c < 1$ and $n \leq 3$. The goal in exploring such a fractal was to find the values of n and c such that the now modified Koch curve is a simple curve and therefore *self-avoiding* [6, p. 124]. *Self-avoiding* curves are continuous lines that do not overlap at any point. In other words, how can they compute n and c so that an (n, c) - von Koch curve does not have overlapping images after it has been iterated Figure 3?

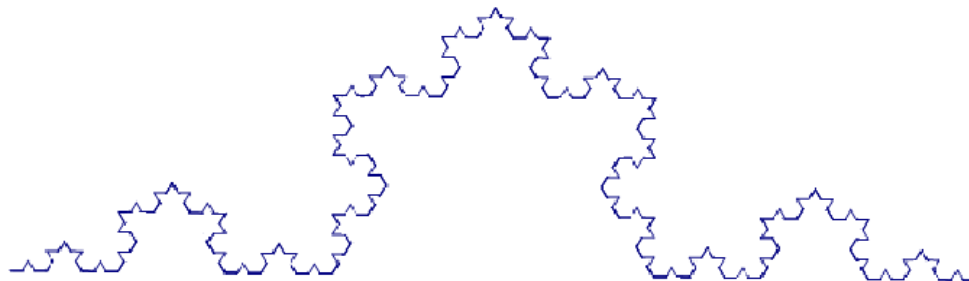


Figure 1. The classical von Koch curve.

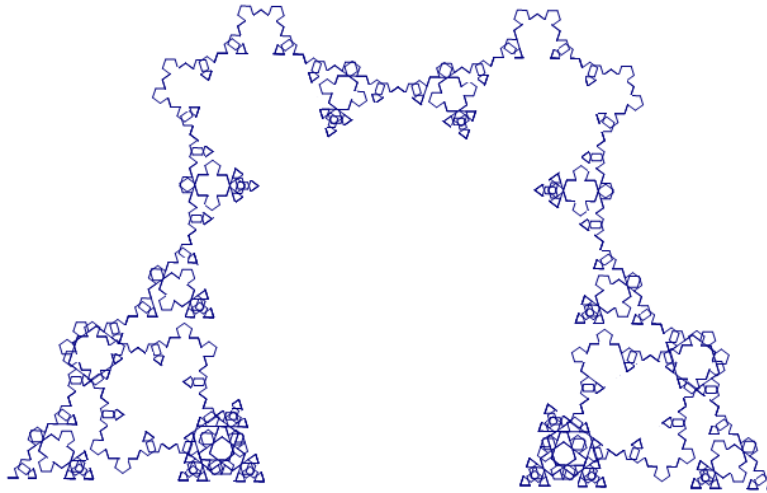


Figure 2. The $(5, 0.20)$ -von Koch curve.

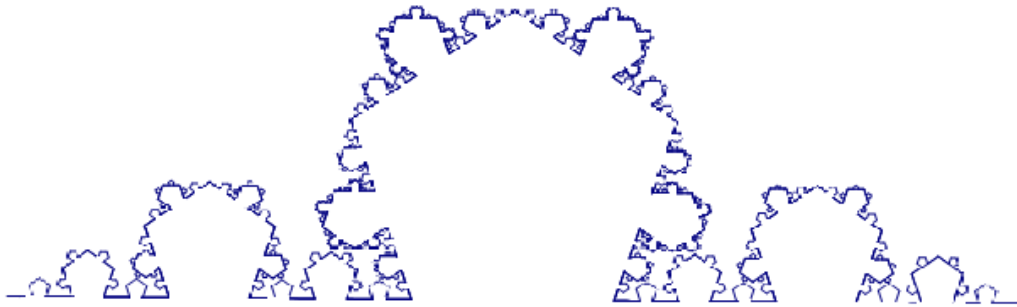


Figure 3. The $(5, \overline{0.33})$ -von Koch curve.

As seen in Figure 2, the iterations in the $(5, 0.20)$ -von Koch curve are overlapping and therefore, self-intersecting. Note that the $n = 5$ is for a 5-gon and $c = 0.20$ is for the base of the parent 5-gon taking up 20% of the base segment. Figure 3, on the other hand is a $(5, \overline{0.33})$ -von Koch curve and is not a self-intersecting curve.

Whether a (n, c) -von Koch curve is self-avoiding or self-intersecting it is still a self-similar set and has finitely many contractive similarities, where each $n+1$ similarity is mapped to one of the $n+1$ resultant line segments. This characteristic maintains an outward oriented curve that is said to have $n+1$ children. *Children* refers to the smaller self-similar protrusions along the curve that are created via iteration. Computing the dimension of a self-avoiding (n, c) -von Koch curve is simple to calculate using the following equation (1), where s is unique and positive

$$(n-1)c^s + 2\left(\frac{1-c}{2}\right)^s. \quad (1)$$

On the other hand, if the (n, c) -von Koch curve is self-intersecting, the dimension is very difficult to calculate, but if $s < 2$ it is expected to be calculated the same as the self-avoiding (n, c) -von Koch curve. Van den Berg studied the $(4, c)$ -von Koch curve and found it to be self-avoiding as long as $c < \frac{1}{3}$. He still wanted to find a critical value for c for any value of n .

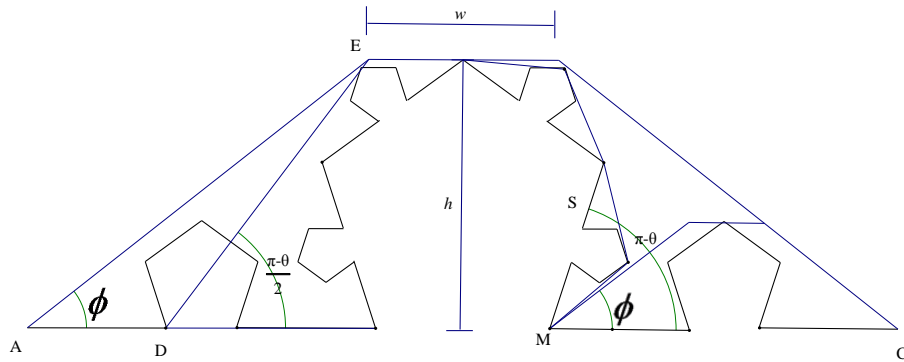


Figure 4. The odd- n (n, c) -von Koch curve approximates an isosceles trapezoid.

Keleti and Paquette found that there are three properties necessary to show that a curve is self-avoiding. These mathematicians used the fact that an even- n (n, c) -von Koch curve approximates an isosceles triangle and an odd- n (n, c) -von Koch curve approximates an isosceles trapezoid Figure 4. The angle was then defined from the base of the parent even- n -gon to the top vertex of the adjacent primary child to be ϕ and the angle created by the base segment and the intersecting side of the even- n -gon to be $\pi - \theta$. The self-avoiding curve of an even- n (n, c) -von Koch curve could then be satisfied when,

$$\pi - \theta > 2\phi.$$

which is equivalent to

$$c < \frac{1}{2 \tan^2(\theta / 2) + 1}.$$

The same angles were used in the odd- n (n, c) -von Koch curve, with an additional angle from the far intersection of the base and the primary child on the left, to the top left vertex of the trapezoid being equal to

$$\frac{\pi - \theta}{2}.$$

The same as with an even- n (n, c) -von Koch curve; the self-avoiding property could be satisfied when

$$\pi - \theta > 2\phi.$$

This has a different outcome with,

$$c < 1 - \sin\left(\frac{\theta}{2}\right).$$

This brief look at (n, c) -von Koch curves has shown a few fairly simple examples of fractals and their construction, but as we delve further into the exploration of these strange “monsters” they will become increasingly more complex and difficult to compute.

Chapter 4: Methods of Measuring Fractal Dimensionality

Before trying to measure a surface's dimension, it is first important to understand what the measurement means. When measuring a surface that is extremely smooth, its surface dimension will approach $D_3 = 2$ and as a surface becomes extremely rough its surface dimension will approach $D_3 = 3$. In other words, moving from a smooth surface to a rough surface can have an infinite number of dimensions between two dimensional to three dimensional structures [2, p. 97].

Data from surfaces such as glass, metal, plastic etc. was traditionally collected using a *stylus profilometer*, which is similar to an old record player needle but is an extremely fine stylus in comparison [4, p. 3]. Using modern technologies such as scanners, lasers or white light from an optical fiber now permits a more extensive, clear and ultimately more accurate analysis of a surface's fractal dimension. Fractal dimension uses include measuring not only glass, metal and plastic surfaces, but also the surface dimension of water, atmosphere, the ocean floor, forest canopies and more.

One tool used to measure dimensionality is the Lipschitz-Killing curvatures or more simply, the LKCs that are quantified as $N+1$ dimensional sets. These measures are used to find limits, volumes and areas of large class similar sets and are a probabilistic part of stochastically self-similar random sets [8, p.2663]. According to Adler, LKCs N -dimensional set A is denoted by $L_0(A), \dots, L_N(A)$ and measures surfaces

of j -dimensional sizes of A [1, p. 810]. For example, when $N = 2$ these dimensions have the following meanings:

$L_2(A)$ is the two dimensional area of A .

$L_1(A)$ is the half boundary length of A .

$L_0(A)$ is the Euler characteristic of A , which in two dimensions is given by

$$L_0(A) = \# \{\text{connected components of } A\} - \# \{\text{holes in } A\}.$$

And when $N = 3$,

$L_3(A)$ is the three dimensional volume of A .

$L_2(A)$ is half the surface area of A .

$L_1(A)$ is twice the caliper diameter of A , where the caliper diameter of a convex A is defined by placing the solid between two parallel planes and finding the mean of the rotations around A . For example, if the planes are rotating around a sphere, then the caliper diameter will be the diameter of the sphere, but if the planes are rotating around a rectangular prism of size $(a \times b \times c)$ it is then, $\frac{(a+b+c)}{2}$, which is half the volume used by airlines to measure the size of passengers' luggage. And again $L_0(A)$ is the Euler characteristic of A , which in three dimensions is given by,

$$L_0(A) = \# \{\text{connected components of } A\} - \# \{\text{handles in } A\} + \# \{\text{holes in } A\}.$$

While handling a random field where the distributional structure is known, but the parameters are unknown, standard statistical techniques for estimating the means and

variances of the random fields are denoted as $C(x, y) = E\{f(x)f(y)\}$. It is also important to note that all non-zero means have been removed from f and so that when f is stationary the notation $C(x, y) \equiv C(x, y)$. Then for the excursion probability for large u when f is stationary and Gaussian,

$$P\left\{\sup_{x \in M} f(x) \geq u\right\} \quad (2)$$

so that the error is

$$\left|P\left\{\sup_{x \in M} f(x) \geq u\right\} - E\{L_0(A_u(f, M))\}\right| \leq error(u). \quad (3)$$

The expressions (2) and (3) provide the necessary tool for estimating the unknown parameters for the LKCs of the excursion sets.

The result of integral geometry known as Steiner's formula is one way used to define the Lipschitz-Killing curvatures. Steiner's formula deals with the N -dimensional volume of enlargements of sets, where the enlargement, resembling a tube of diameter $p > 0$ is built around the set of $A \in \mathbb{R}^N$ such that it is the set

$$Tube(A, p) = \{x \in \mathbb{R}^N : \min\|x - y\| \leq p\}$$

showing the minimal distance.

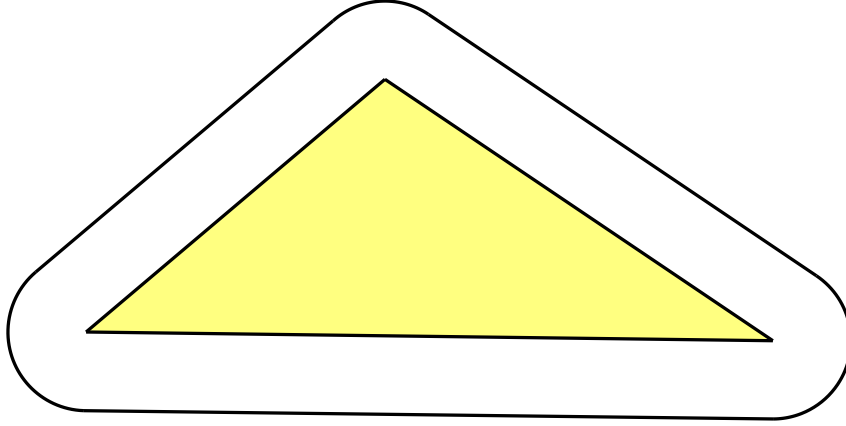


Figure 5. The tube around a triangle.

Figure 5, represents a solid triangle, A , with a $Tube(A, \rho)$ that is larger than the triangular region and has rounded corners. It is important to notice that $Tube(A, \rho)$ always includes triangle A and has rounded corners giving the appearance of a solid tube. The tubes then create a volume to the surface and make it possible to measure the dimension of the surface dimension of a given object [1, p. 814].

Steiner's theorem further states that if λ_N represents the volume in \mathbb{R}^N , then, for convex A of dimension $\dim(A)$,

$$\lambda_N(Tube(A, \rho)) = \sum_{j=0}^{\dim(A)} \omega_{N-j} \rho^{N-j} L_j(A),$$

where $\omega_j = \frac{\pi^{j/2}}{\Gamma(1 + j/2)}$ is the volume of the unit sphere in \mathbb{R}^3 as previously described

thus, the LKCs satisfy a basic scaling relationship, $L_j(\lambda A) = \lambda^j L_j(A)$, for $0 \leq j \leq \dim(A)$

and $\lambda > 0$, where $\lambda A = \{x : x = \lambda y, \text{ for some } y \in A\}$. Showing that $L_j(A)$ is the measure of the j -dimensional volume of A .

Another set of geometrical tools related to the LKCs is the Gaussian Minkowski functionals. Gaussian fields in general will be more fully addressed later in this paper. The Minkowski functionals are related to the hitting set of f in D and over M as defined by

$$A_D \equiv A_D(f, M) \triangleq \{x \in M : f(x) \in D\} \quad (4)$$

where D is the set $[u, \infty)$.

Instead of measuring the basic Euclidean sizes of the hitting sets, however, the aspect of the Gaussian probability content is measured. This lets X be a vector of k independent and identically distributed standard Gaussian random variables so that set $A \in \mathbb{R}^k$ is written as

$$\gamma_k(A) = P\{X \in A\} = \int_A \frac{e^{-\|x\|^2/2}}{(2\pi)^{k/2}} dx.$$

The above equation actually defines the tubes the same as before, but now there is a Taylor expansion for the probability content of tubes that is written as

$$\gamma_k(\text{Tube}(A, \rho)) = \sum_{j=0}^{\infty} \frac{\rho^j}{j!} \mathcal{M}_j^k(A),$$

for small enough ρ . Now we can say that the coefficients $\mathcal{M}_j^k(A)$ are the Gaussian Minkowski functionals or GMFs of A, such that $\mathcal{M}_0^k(A) = \gamma_k(A)$. The GMFs differ from the Steiner's theorem in that it is an infinite expansion. So let $k = 1$ and $A = [u, \infty)$, then

$$\gamma_1(\text{Tube}([u, \infty), \rho)) = \gamma_1([u - \rho, \infty)) = \psi(u - \rho),$$

where,

$$\psi(u) = (2\pi)^{-1/2} \int_u^\infty e^{-x^2/2} dx$$

is the tail probability function for a standard Gaussian variable. Some may find it more familiar as the volume under the curve of the normal distribution function as it is rotated around its vertical axis.

Gaussian fields are the basic fields used since they allow for both univariate and multivariate distributions to be normal. In the real-valued case, $f : M \rightarrow \mathbb{R}$ and has the property that all collections $f(x_1), \dots, f(x_2)$, of random variables will have multivariate Gaussian distributions for all $k \geq 1$ and all $x_1, \dots, x_k \in M$.

The random field, $f : M \rightarrow \mathbb{R}^d$ to find a vector valued Gaussian random field,

$$g(x) = (g_1(x), \dots, g_k(x)) : M \rightarrow \mathbb{R}^k,$$

has independent and identically distributed components having zero means and unit variances and a function

$$F : \mathbb{R}^k \rightarrow \mathbb{R}^d,$$

such that f has the same multivariate distributions as $F(g)$.

Now when F is not invertible, $f = F(g)$ provides a qualitatively different value from g , with three methods for F ,

$$\sum_1^k x_i^2 \quad (5)$$

$$\frac{x_1 \sqrt{k-1}}{\left(\sum_2^k x_i^2\right)^{1/2}} \quad (6)$$

$$\frac{m \sum_1^n x_i^2}{n \sum_{n+1}^{n+m} x_i^2} \quad (7)$$

where, $k = n + m$.

The χ^2 fields previously discussed have k degrees of freedom and the F field has n and m degrees of freedom. Additionally, it is important to note that there is no transformation of the three fields, (5), (6) and (7) that can transform them into real valued Gaussian fields. So that the Gaussian related field f of the excursion sets A_D is rewritten as

$$\begin{aligned} A_D(f, M) &= A_D(F(g), M) \\ &= \{x \in M : (F \circ g)(t) \in D\} \\ &= \{x \in M : g(x) \in F^{-1}(D)\} \\ &= A_{F^{-1}(D)}(g, M). \end{aligned}$$

This shows that the excursion set of a real valued non-Gaussian $f = F \circ g$, is equivalent to the excursion set for vector valued Gaussian g in $F^{-1}([u, \infty)) \in \mathbb{R}^k$.

Chapter 5: Chaotic Dynamical Systems

The real world is full of many dynamic systems such as weather, geography, plant structures and more. Often, these systems seem to be random with no predictable outcomes, when in fact these systems are anything but random. This is where a strong definition of *chaos* is needed. Making predictable sense of a seemingly random system is an informal way of defining chaos. DeVaney defines chaotic dynamical systems such that,

$f : J \rightarrow J$ is said to be topologically transitive if for any pair of open sets $U, V \subset J$ there exists $k > 0$ such that $f^k(U) \cap V \neq \emptyset$,

where k is an integer and

$f : J \rightarrow J$ has sensitive dependence on initial conditions if there exists $\delta > 0$ such that, for any $x \in J$ and any neighborhood N of x , there exists $y \in N$ and $n \geq 0$ such that $|f^n(x) - f^n(y)| > \delta$,

where n is an integer.

In other words, for a system to be chaotic, it must be able to map onto a dense orbit and is sensitive to initial conditions [7, p. 49].

An important part of any chaotic system is to identify the *fixed points* of the system. *Fixed points* are simply the points in a system that seed values are attracted to or repelled from under iteration so that $f(a) = a$.

To find fixed points of $f(x)$, let $I = [a, b]$ and let $f : I \rightarrow I$ be a continuous function. Then set the function equal to x . The following proof illustrates the fact that f has at least one fixed point in I [3].

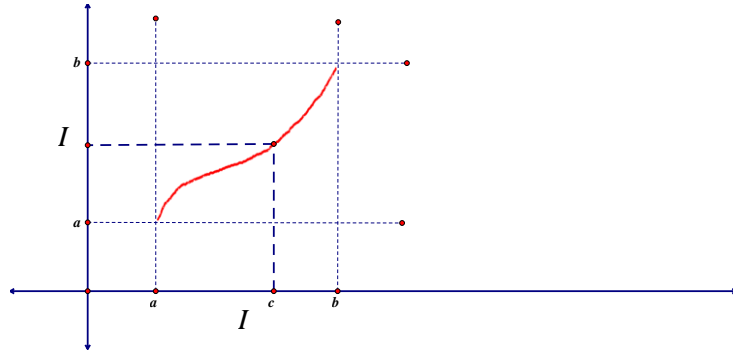


Illustration 4. Drawing that represents one fixed point in I .

Proof: given $f(x) = x$ and $g = f(x) - x$ let $\varepsilon > 0$ and $I = [a, b]$ such that $f : I \rightarrow I$. And by the intermediate value theorem (IVT), $\exists c \in I$ such that $a \leq c \leq b$ and $f(c) = z$. Then because f is continuous $f(a) > a$ so, $f(a) - a \geq 0$ and $g(a) = f(a) - a$. Similarly, $f(b) - b < 0$ since $f(b) < b$. Now, if $g(a) > 0$ then $g(b) < 0 < g(a)$. Then by IVT there exists a point p where $a \leq p \leq b$ such that $g(p) = 0$. It is known that $g(p) = f(p) - p$ so, $0 = f(p) - p$ which means that $f(p) = p$. This shows that f has at least one fixed point on I . *QED*

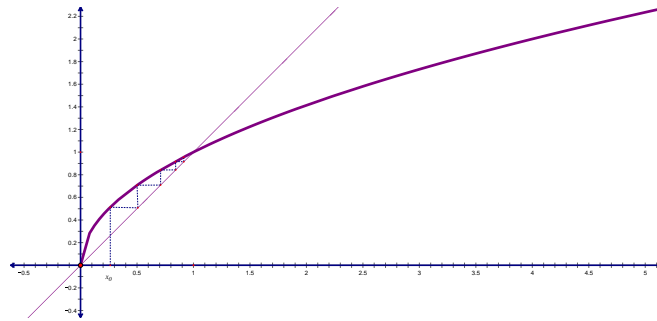


Illustration 5. Drawing that represents an attracting fixed point.

Once the fixed points are found, then the attracting properties of the fixed points can be investigated. If $|F^n(x_0)| < 1$, then the fixed point will be an attracting fixed point and if $|F^n(x_0)| > 1$, then the fixed point will be a repelling fixed point.

Another important part of chaos is the transformation of figures in the complex-plane. An example of a transformation of a circle in the complex-plane with a radius of one unit and its center at $(1+0i)$ will be shown.

The function

$$f(z) = z^2$$

where

$$z = a + bi$$

will be applied to the circle to create the transformation. Also, Euler's Formula

$$e^{i\alpha} = \cos \alpha + i \sin \alpha$$

will be used to complete this transformation on a set of key points in the circle, then the properties of the transformation will be used to estimate where to fill in the rest of the resulting figure [3].

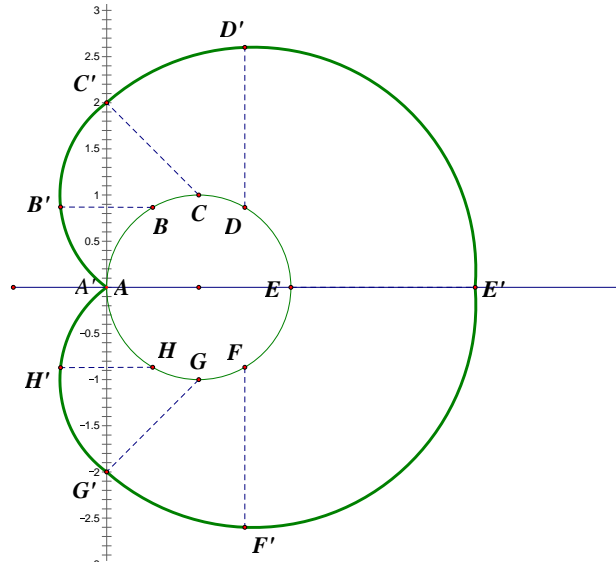


Figure 6. Cardioid formed by applying $f(z) = z^2$ to a circle.

Using Euler Numbers in the complex function $f(z) = z^2$, one can now write f in the form

$$f(z) = r^2 e^{i2\alpha}.$$

where r is the modulus of a given complex number z and α is the angle associated with z . Referring to Figure 6, point A is at $(0+0i)$. The distance from the origin is zero and the angle from the origin is zero so,

$$f(z)_A = 0^2 e^{i2*0} = 0$$

This places A' right back at the origin. Point C is at $(1+1i)$ which is $\sqrt{2}$ from the origin at an angle of $\frac{\pi}{4}$ so,

$$f(z)_{C'} = \sqrt{2}^2 e^{i2\frac{\pi}{4}} = 2i$$

placing C' at $(0+2i)$. Point G is the same distance from the origin with an angle of $-\frac{\pi}{4}$ so G' is a reflection of C' at $(0-2i)$. Now point E at $(2+0i)$ is 2 from the origin and has an angle of zero so,

$$f(z)_E = 2^2 e^{i2*0} = 4$$

placing E' at $(4+0i)$.

Using Euler Numbers made the task of finding these four key points of transformation relatively simple. The points B , D , F and H will be found in the same manner. Plotting these additional four points will allow a more accurate estimation when filling in the rest of the curve by hand.

The resulting figure is called a *cardioid* due to its heart shaped appearance, which is the foundational shape of the Mandelbrot set as previously seen in Illustration 2. From here it is now easy to see that the Mandelbrot set was created by transforming $f(z) = z^2$ to $f(z) = z^2 + c$ and applying this new equation to the transformation of a circle in the complex plane.

Chapter 6: Conclusion

This report has given a brief overview of just a few fractals and how they are constructed and utilized. It proposes that both beautiful and practical fractals are equally valuable to the mathematical community and to many other groups as well. Fractal theory is employed in art, finance, ecology, geography and much more.

The calculation of a system's dimensionality was addressed as well as the potential uses for dimensional measures. One can no longer look at complex and chaotic systems in a traditionally discrete 1, 2 or 3 dimensional manner as with Euclidean Geometry. An image can take infinitely many dimensions ranging from 1 to 2. Likewise a surface is likely not to be smooth enough to be considered strictly 2 dimensional, because the subtle self similar bumps and crevices give surfaces a dimension somewhere between 2 and 3.

The modified n -gon Koch's curve gives insight into a new way of creating and exploring fractals transformed from a well know model. The investigation of this curve utilizes constructions and processes used to calculate the dimensionality of fractals.

The topics discussed in this report could easily be imbedded into secondary mathematics lessons in Geometry, Algebra 1 or 2 and of course Precalculus. Students would benefit from learning recursive notation and how to use iteration and function compositions to solve problems as simple as linear models all the way to restricted exponential growth models.

References

1. Adler, Robert J, Some new random field tools for spatial analysis, *Stoch Environ Res Risk Assess*, 22 (2008) 809-822.
2. Constantine, AG, Peter Hall, Characterizing surface smoothness via estimation of effective fractal dimension, *Journal of the Royal Statistical Society*, 56 (1994) 97-113.
3. Daniels, Mark, M396C-Discrete Deterministic Chaos (92445), University of Texas, 2011
4. Davies, Steve, Peter Hall, Fractal analysis of surface roughness by using special data, *Journal of the Royal Statistical Society*, 61 (1999) 3-37.
5. DeVaney, Robert L., *A First Course in Chaotic Dynamical Systems*, Addison-Wesley Publishing Company, Inc, Menlo Park, 1992.
6. Keleti, Tamas, Elliot Paquette, The Trouble with von Koch Curves Built from n-gons, *The Mathematical Association of America*, 117 (2010) 124-136.
7. Stevens, Roger T., *Creating Fractals*. Charles River Media, Inc, Hingham, 2005.
8. Zahle, M, Lipschitz-Killing curvatures of self-similar random fractals, *American Mathematical Society*, 363 (2011) 2663-2684.

Vita

Jodi Lynette Wheeler graduated *cum laude* from The University of Texas in San Antonio with a B.S. in Mathematics and a Minor in Statistics. She has taught various mathematics courses at Stevens High School since 2006, to include Algebra 1, Geometry and Advanced Mathematical Decision Making (now known as Advanced Quantitative Reasoning). As of 2011, she has been promoted to the Math Coordinator at Stevens High School. Jodi currently resides in San Antonio, Texas with her husband David and her three sons Samuel, Stewart and Isaac.

Email address: jodi.wheeler@nisd.net

This report was typed by Jodi Lynette Wheeler.